IEEE Access
Multidisciplinary | Rapid Review | Open Access Journal

SPECIAL SECTION ON ADVANCED INTERNET OF THINGS FOR SMART CYBER-PHYSICAL INFRASTRUCTURE SYSTEMS

Received January 26, 2021, accepted February 25, 2021, date of publication March 12, 2021, date of current version April 2, 2021.

Digital Object Identifier 10.1109/ACCESS.2021.3065564

A Multi-Iteration Enhanced 2P-SMA Method for Improved Error Reduction on a WP-SAW Water Temperature and Pressure Sensor

ZHAOZHAO TANG[1,2], WENYAN WU[3], JINLIANG GAO[4], JINGTING LUO[1], RAN TAO[1], CHEN FU[1], AND LUOYUN XU[5,6]

[1]Key Laboratory of Optoelectronic Devices and Systems, College of Physics and Optoelectronic Engineering, Shenzhen University, Shenzhen 518060, China
[2]School of Computing and Digital Technologies, Staffordshire University, Stoke-on-Trent ST4 2DE, U.K.
[3]School of Engineering and the Built Environment, Birmingham City University, Birmingham B4 7XG, U.K.
[4]School of Environment, Harbin Institute of Technology, Harbin 150090, China
[5]Huadian Electric Power Research Institute, Hangzhou 310030, China
[6]College of Electrical Engineering, Zhejiang University, Hangzhou 310007, China

Corresponding authors: Jingting Luo (luojt@szu.edu.cn) and Chen Fu (chenfu@szu.edu.cn)

This work was supported in part by the National Key Research and Development Program of China under Grant 2016YFB0402705; in part by the National Natural Science Foundation of China under Grant 11704261, Grant 11974252, Grant 51605485, and Grant 11575118; in part by the Shenzhen Science and Technology Project under Grant JCYJ20170817100658231, Grant JCYJ20180305124317872, Grant JCYJ20180507182106754, and Grant JCYJ20180507182439574; in part by the China Postdoctoral Science Foundation under Grant 2019M653018; in part by EU FP7–ICT–WatERP under Grant 318603; and in part by the EU FP7 Marie Curie Actions–SmartWater under Grant 318985.

ABSTRACT Due to the instability of the characteristics of materials, fabrication processes and user handling, newly designed and fabricated wireless passive surface acoustic wave (WP-SAW) sensor nodes have inconsistent sensing performance. Furthermore, ambient environmental interferences aggravate inconsistences under complex working conditions. In this paper, a multi-iteration enhanced two-point simple moving average (MI-2P-SMA) method is proposed for sensing error reduction of a WP-SAW reflective delay line water temperature and pressure sensor. This method is improved from the traditional 2P-SMA method for better performance on error reduction. The results show: the MI-2P-SMA method does not change the original characteristics of experimental data; it can reduce relative errors of the WP-SAW reflective delay line water temperature and pressure sensor and has better performance than a traditional 2P-SMA method; it reduces the number of data points and the extent of this reduction is dependent on iteration time.

INDEX TERMS Multi-iteration, two-point simple moving average, error reduction, temperature, pressure, surface acoustic wave, sensor.

I. INTRODUCTION

The demand of sensors is growing rapidly worldwide. Besides the growth of the quantity, the technical requirements for better performance of sensors and the demand of customed sensing systems from industrials are increasing greatly due to the development of Internet of Things (IoT) enabled technologies [1]–[6]. Wang *et al.* [1] proposed an intelligent trust evaluation scheme in sensor-cloud-enabled industrial IoT. Qi *et al.* [2], [3] reviewed data fusion techniques for IoT applications and IoT for healthcare systems, and did researches on IoT enabled wearable sensors. Astill *et al.* [4] reviewed smart sensors, big data, and IoT for smart poultry management. Kamilaris and Pitsillides [5] reviewed IoT in mobile phone computing. Liu *et al.* [6] reviewed spintronic sensors with Internet of Things for smart living.

Wireless passive surface acoustic wave (WP-SAW) sensors have been increasingly investigated by worldwide researchers nowadays. It is so attractive because of its passive characteristics which makes batteries unnecessary in sensing systems, outstanding stability and reliability in harsh environment, small size making it easy to deploy for various applications, and its investor-friendly low cost [7]–[14].

WP-SAW sensors have been developed for measuring different kinds of physical quantities such as temperature [15], pressure [16], toque [17], strain [18], etc. and gas densities such as NO_2 [19], CO_2 [20], etc. However, the sensing data obtained and processed by newly designed and fabricated

The associate editor coordinating the review of this manuscript and approving it for publication was Po Yang.

sensors are affected by errors due to various interferences, e.g., characteristics of materials, vibration effect, chip integration orientation misalignment, heating issues, random noise of operating environment, handling of world users, etc. [21]–[25].

Researchers made efforts on reduction of sensing errors caused by these interferences. Some algorithms were developed by previous researchers [26], such as least squares [27], polynomial fitting [28], and interpolation [29], etc., but these methods do not reflect real-time output data and cannot be used for real-time monitoring tasks. This disadvantage limits their usage scenarios. A traditional two-point simple moving average has very limited effect on error reduction on sensing errors if the variance is not close to 1 [30].

In order to resolve the aforementioned problem, an improved multi-iterative two-point simple moving average (MI-2P-SMA) method is proposed in this paper. For verification of its characteristics and effectiveness, it is applied to the original experimental sensing data of a newly designed and fabricated WP-SAW reflective delay line temperature and pressure sensor.

This research makes the following contributions.

1) The improved MI-2P-SMA is derived mathematically from the traditional 2P-SMA and analyzed using a diagram.

2) The improved MI-2P-SMA is successfully utilized to reduce relative errors on a WP-SAW reflective delay line temperature and pressure sensor.

3) The limitations of the improved MI-2P-SMA are summarized that the iteration time is limited to keep the characteristics of original data and at least half data points.

The rest paper is organized as follows. In Section II, the mathematical derivation of the improved MI-2P-SMA is presented. It is derived from the fundamental SMA theory and improved from the traditional 2P-SMA. It is described by a mathematic equation and a diagram. An architecture of data flow is proposed to explain how the MI-2P-SMA method works. In Section III, the WP-SAW reflective delay line temperature and pressure sensor is introduced. In Section IV, the experiments for obtaining sensing data are presented. In Section V, experimental data are compared with the data after MI-2P-SMA is applied. Regression and relative error analysis are utilized for data analysis. Finally, in Section VI, the results are concluded.

II. MULTI-ITERATION ENHANCED TWO-POINT SIMPLE MOVING AVERAGE

A. MATHMATICAL DERIVATION

SMA can be utilized to reduce random noise and retain a sharp step response. It operates by averaging a series of points from input to produce each point in the output signal, which can be described as (1).

$$y(i) = \frac{1}{M}\sum_{j=0}^{M-1} x(i+j) \tag{1}$$

where x is the input signal; y is the output signal; M is the number of points in average; i is the order of the data.

Therefore, a 2P-SMA is that the number of points in average is 2, which is described as (2).

$$y_1(i) = \frac{x(i) + x(i+1)}{2} \tag{2}$$

If the output of this 2P-SMA is the input of another 2P-SMA process, this entire two-step process is defined as a 2-iterative 2P-SMA, which can be described as (3).

$$y_2(i) = \frac{y_1(i) + y_1(i+1)}{2} = \frac{x(i) + 2x(i+1) + x(i+2)}{4} \tag{3}$$

If this goes further, an n-iterative 2P-SMA process can be concluded and described as (4).

$$\begin{aligned} y_n(i) &= \frac{C_n^0 x(i) + C_n^1 x(i+1) + C_n^2 x(i+2) + \ldots + C_n^n x(i+n)}{2^n} \\ &= \frac{1}{2^n}\sum_{j=0}^{n} C_n^j x(i+j) \end{aligned} \tag{4}$$

where n is a natural number; C_n^0, C_n^1, C_n^2, $\ldots$, C_n^n are combinations, which are defined as (5).

$$C_n^k = \frac{n!}{k!\,(\text{n-k})!} \tag{5}$$

where k is a natural number and less or equal to n, and $n!$, $k!$, and (n-k)! are factorials.

Equation (4), an n-iterative 2P-SMA, is defined as an n-time MI-2P-SMA. Actually, the traditional 2P-SMA is a one-time MI-2P-SMA.

B. DIAGRAM AND ANALISIS

Figure 1 is the diagram of the MI-2P-SMA, which shows the data flow and also some features of the MI-2P-SMA. The feathers of MI-2P-SMA are summarized as follows. The first row shows the i-th point and its subsequent points of original data before MI-2P-SMA is applied, and the number of points of this row is $m + 1$. y_n is the $(n + 1)$-th row which is the i-th point and its subsequent points of original data after n-time MI-2P-SMA. The number of original data points reduces n after n-time MI-2P-SMA.

C. ITERATION TIME

In order to improve the accuracy of sensing systems, MI-2P-SMA is applied to the original experimental data. However, the iteration time n should be limited to an appropriate range because of the feature of the reduction of data points. In order to have effective number of data points to keep characteristics of the original data, $m + 1$ must be much larger than n. To select appropriate iteration time n is a key issue for the best performance of MI-2P-SMA.

Figure 2 shows the flow chart to select appropriate iteration time n. This flow chart proposes the methodology to obtain the n. Firstly, the characteristic curve section of original data Result (0) needs to be indicated. The characteristic curve

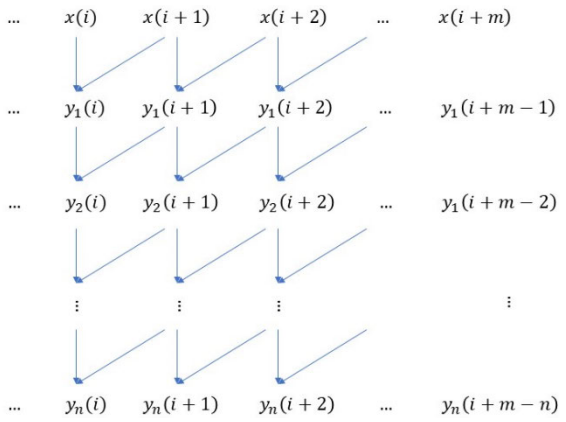

FIGURE 1. The diagram of the MI-2P-SMA.

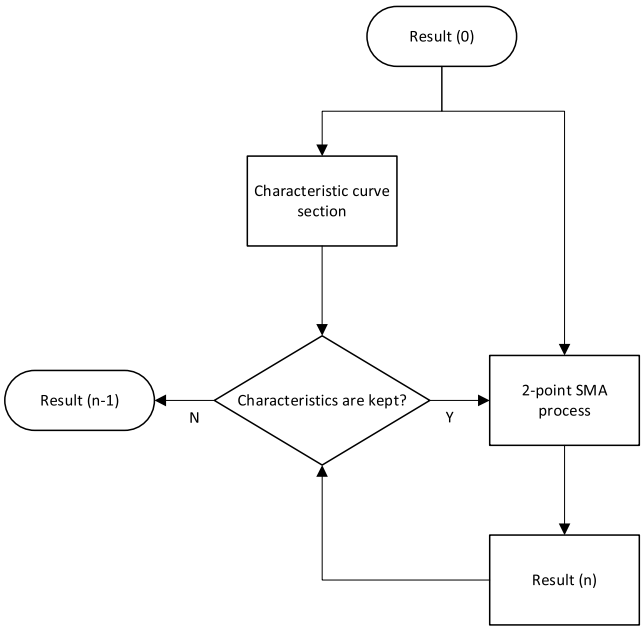

FIGURE 2. The flow chart to select the iteration time.

section is the core section of the curve which represents the characteristics of the data and cannot be omitted. Then 2-point SMA is applied to Result (0) to obtain the 1-time MI-2P-SMA result Result (1). Compare the curve of Result (1) with the characteristic curve section and judge if the curve of Result (1) keeps the characteristics of the characteristic curve section. If the curve of Result (1) keeps the characteristics, apply 2-point SMA to Result (1) and obtain Result (2) and do the aforementioned check again. This loop works until the curve of Result (n) does not keep the characteristics, make the Result ($n-1$) final result, where n is a natural number. Result (n) is the result of n-time MI-2P-SMA.

III. WP-SAW WATER TEMPERATURE AND PRESSURE SENSOR

The newly designed and fabricated WP-SAW sensor node is a WP-SAW reflective delay line temperature and pressure sensor node fabricated on a 0.5 mm thick Y-Z cut $LiNbO_3$ piezoelectric crystal substrate, which has been presented in our previous work [31]–[33]. Table 1 shows the parameters of this WP-SAW sensor, and Figure 3 shows the structure of this WP-SAW sensor node.

TABLE 1. Parameters of the WP-SAW reflective delay line temperature and pressure sensor node.

Component name and unit	Parameters
Centre frequency (MHz)	433
SAW wavelength λ (μm)	8
Bar width (μm)	2
Bar interval (μm)	2
Bar length (μm)	440
IDT diameter (μm)	400
Thickness of metal Al (μm)	0.2
Distance between IDT and R_1 (μm)	7000
Distance between IDT and R_2 (μm)	2400
Distance between IDT and R_3 (μm)	4800

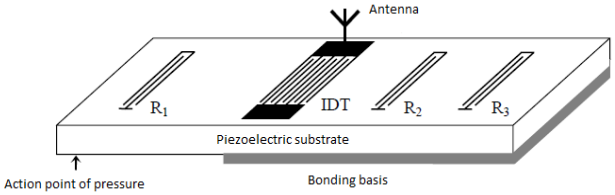

FIGURE 3. The structure of WP-SAW reflective delay line temperature and pressure sensor node [31]–[33].

An IDT is fabricated in the center of the surface of the substrate for converting received RF signals to the energy of SAW, and also re-converting the reflected SAW energy back to RF signals. The antenna is connected to the IDT for interrogation RF signal receiving and response signal transmission. The SAW propagates on the surface of the substrate, which is vertical to the IDT bars and to both opposite directions from the IDT. Three reflectors are fabricated on the surface of the substrate on the way of SAW propagation, which are paralleled to the IDT. Sound absorption materials are applied to the edges of the substrate for absorbing redundant SAW energy to avoid interferences on the useful SAW reflections. In Fig. 3, one reflector R_1 is on the left side of the IDT for pressure sensing purpose, and two reflectors R_2 and R_3 are on the right side of the IDT for temperature sensing purpose. On the left side of the IDT, the substrate acts as a cantilever on which ambient pressure change acts on it to make deformation to the left side of the substrate. This leads to the change of the distance between R_1 and the IDT, and subsequently influences the SAW propagation to make time delay change for sensing purpose. On the right side of the IDT, the substrate is bonded to the package to sense the temperature change. The temperature change can also make deformation of the substrate to make SAW propagation change which further causes the time delay change.

This WP-SAW reflective delay line temperature and pressure sensor has the following regulations based on our previous work [30]. In time domain, phase differences of the response signals reflected by the three reflectors from the

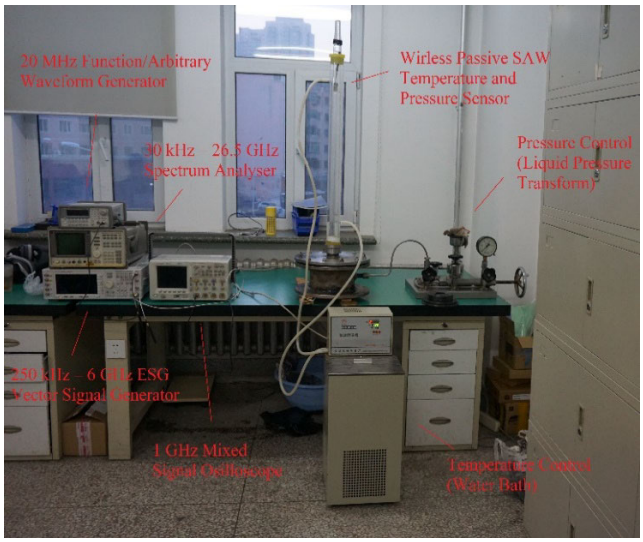

FIGURE 4. The photo of the experimental framework and instruments for testing the fabricated WP-SAW reflective delay line temperature and pressure sensor node [31]–[33].

sensor node have linear relationships with testing temperature and pressure changes, which can be shown in (6) and (7).

$$T - T_i = A\,(\varphi_3 - \varphi_{3i}) \tag{6}$$

$$P - P_i = B(\varphi_1 - \varphi_{1i}) - C(T - T_i) \tag{7}$$

where T_i is the initial temperature and φ_{3i} is the corresponding initial phase difference of the response signal reflected by R_3; T is the temperature and φ_3 is the corresponding phase difference of the response signal reflected by R_3; A is a constant related to the wavelength of the SAW, the substrate material and the distance between the IDT and R_3. Similarly, P_i is the initial pressure and φ_{1i} is the corresponding initial phase difference of the response signal reflected by R_1; P is the Pressure and φ_1 is the corresponding phase difference of the response signal reflected by R_1; B is a constant related to the wavelength of the SAW, the substrate material and the distance between the IDT and R_1; C is a constant related to the substrate material.

IV. EXPERIMENTS

Figure 4 shows the photo of the experimental framework for testing the fabricated WP-SAW reflective delay line temperature and pressure sensor node. The instruments include an Agilent 33220A Function/Arbitrary Waveform Generator (20 MHz), an Agilent E4438C ESG Vector Signal Generator (250 kHz – 6 GHz), an Agilent MSO 6104A Mixed Signal Oscilloscope (1 GHz) and an Agilent E4440A PSA Series Spectrum Analyzer (30 kHz – 26.5 GHz). The sensor node is placed in the inner layer top of a double-layer glass pipe. The inner layer of the pipe is strictly sealed by the steal substrate and have access to the liquid pressure transfer platform for pressure test purpose. The outer layer of the pipe is sealed by a rubber plug and connected to the water bath temperature controller by two rubber hoses for a water cycle to control the temperature of the inner layer pipe. The sensor node receives

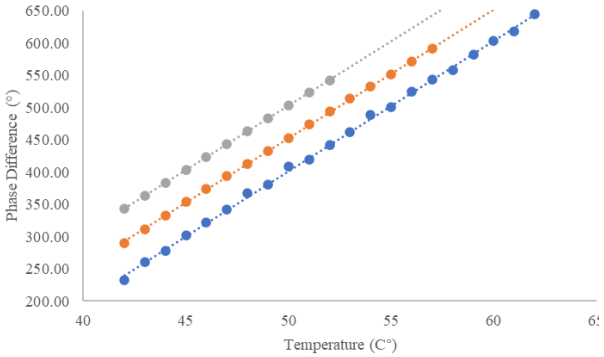

FIGURE 5. The comparison of original experimental data, 5-, and 10-time MI-2P-SMA processed data with linear regression analysis: blue – original, orange – 5, grey – 10.

TABLE 2. The linear regression equations and variances of original experimental data, 5-, and 10-time MI-2P-SMA processed data.

Iteration time	Linear regression equation	Variance
0	y = 20.165x - 606.77	0.9991
5	y = 19.982x - 546.55	0.9998
10	y = 19.947x - 494.33	0.9999

the interrogation RF signal which is the wireless modulated signal from the Agilent E4438C ESG Vector Signal Generator, and then reflect it to form response signals with sensing information to the Agilent MSO 6104A Mixed Signal Oscilloscope and Agilent E4440A PSA Series Spectrum Analyzer which are used to record and process both interrogation and response RF signals.

V. RESULTS AND DISCUSSIONS

A. TEMPERATURE DATA

Figure 5 shows the comparison of original experimental temperature data, 5-, and 10-time MI-2P-SMA processed data with linear regression analysis: blue dots and line shows original experimental data and their trend line; orange dots and line shows 5-time MI-2P-SMA processed data and their trend line; grey dots and line shows 10-time MI-2P-SMA processed data and their trend line. Table 2 shows the linear regression equations and variances of original experimental temperature data, 5-, and 10-time MI-2P-SMA processed data, where x is the temperature value and y is the phase difference value. The linear regression equation represents the theoretical linear relation between temperature and the phase difference of the response signal reflected by R_3. The variance values are close to 1, which means the data are close to their linear regression equations.

Relative error can be calculated by (8). Figure 6 shows the comparison of relative errors of original experimental temperature data, 5-, and 10-time MI-2P-SMA processed data. Table 3 shows the range of relative errors of original experimental temperature data, 5-, and 10-time MI-2P-SMA processed data. The range of relative errors of the original experimental temperature data is from −3.40% to 1.87%. After 5-, and 10-time MI-2P-SMA, the range of relative errors

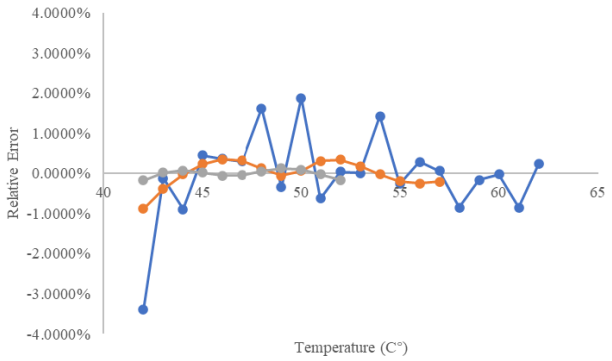

FIGURE 6. The comparison of relative errors of original experimental data, 5-, and 10-time MI-2P-SMA processed data: blue – original, orange – 5, grey – 10.

TABLE 3. The range of relative errors of original experimental temperature data, 5-, and 10-time MI-2P-SMA processed data.

Iteration time	Minimum	Maximum
0	-3.3977%	1.8731%
5	-0.8777%	0.3530%
10	-0.1688%	0.1280%

is from -0.88% to 0.35%, and from -0.17% to 0.13%, respectively.

$$\delta = \frac{\Delta}{L} * 100\% = \frac{Experimental\ value - Theoretical\ value}{Theoretical\ value} * 100\% \quad (8)$$

In summary of temperature data analysis, the MI-2P-SMA method does not change the original characteristics of experimental temperature data. The more iterative times of MI-2P-SMA applies, the range of relative errors is more significantly reduced, and the variance values are closer to 1. This indicates that the more iterative times of MI-2P-SMA applies, the temperature data are closer to their linear regression equations. Figure 5 shows the obvious reduction of the number of data points, which verified the regulation of MI-2P-SMA presented in Section 2. In this temperature data case, the characteristic curve of original experimental temperature data is almost linear. After 10-time MI-2P-SMA, the variance is extremely close to 1; the range of the relative errors is significantly reduced; more than half data points are kept. Therefore, 10 iteration times are selected for this temperature data case.

B. PRESSURE DATA

Figure 7 shows the comparison of original experimental pressure data, 4-, 5-, 6-, and 10-time MI-2P-SMA processed data with linear regression analysis: blue dots and line shows original experimental data and their trend line; orange dots and line shows 4-time MI-2P-SMA processed data and their trend line; grey dots and line shows 5-time MI-2P-SMA processed data and their trend line; yellow dots and line shows 6-time MI-2P-SMA processed data and their trend line; sky blue dots and line shows 5-time MI-2P-SMA processed data and their trend line. Table 4 shows the linear regression equations and variances of original experimental pressure data, 4-, 5-, 6-, and 10-time MI-2P-SMA processed data, where x is the pressure value and y is the phase difference value. The linear regression equation represents the theoretical linear relation between pressure and the phase difference of the response signal reflected by R_1. The variance values are close to 1, which means the data are close to their linear regression equations.

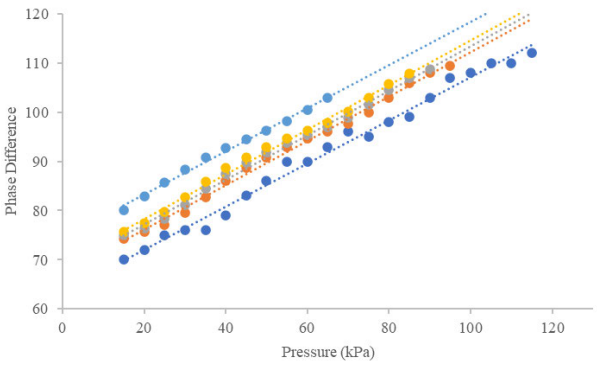

FIGURE 7. The comparison of original experimental pressure data, 4-, 5-, 6-, and 10-time MI-2P-SMA processed data with linear regression analysis: blue – original, orange – 4, grey – 5, yellow – 6, sky blue – 10.

TABLE 4. The linear regression equations and variances of original experimental pressure data, 4-, 5-, 6-, and 10-time MI-2P-SMA processed data.

Iteration time	Linear regression equation	Variance
0	y = 0.4384x + 63.311	0.9896
4	y = 0.4515x + 67.107	0.9946
5	y = 0.4538x + 68.119	0.9947
6	y = 0.4545x + 69.223	0.9945
10	y = 0.4396x + 74.483	0.993

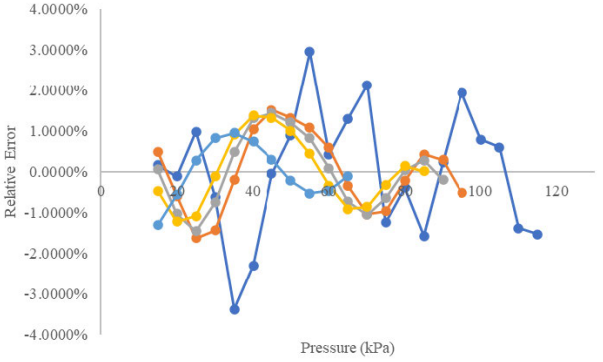

FIGURE 8. The comparison of relative errors of original experimental pressure data, 4-, 5-, 6-, and 10-time MI-2P-SMA processed data: blue – original, orange – 4, grey – 5, yellow – 6, sky blue – 10.

Figure 8 shows the comparison of relative errors of original experimental pressure data, 4-, 5-, 6-, and 10-time MI-2P-SMA processed data. Table 5 shows the range of relative errors of original experimental pressure data, 4-, 5-, 6-, and 10-time MI-2P-SMA processed data. The range of relative errors of the original experimental pressure data is from

TABLE 5. The range of relative errors of original experimental pressure data, 4-, 5-, 6-, and 10-time MI-2P-SMA processed data.

Iteration time	Minimum	Maximum
0	-3.3755%	2.9477%
4	-1.6194%	1.5162%
5	-1.4491%	1.4372%
6	-1.2177%	1.3802%
10	-1.2971%	0.9553%

−3.38% to 2.95%. After 4-, 5-, 6-, and 10-time MI-2P-SMA, the range of relative errors is from −1.62% to 1.52%, from −1.45% to 1.44%, from −1.22% to 1.38%, and from −1.30% to 0.96%, respectively.

In summary of pressure data analysis, the MI-2P-SMA method does not change the original characteristics of experimental pressure data. The more iterative times of MI-2P-SMA applies, the range of relative errors is more significantly reduced, but in this pressure data case, the variance value reaches highest after 5-time MI-2P-SMA, and then it gradually drops. Figure 7 also shows the obvious reduction of the number of data points, which verified the regulation of MI-2P-SMA presented in Section 2. In this pressure data case, the characteristic curve of original experimental pressure data is almost linear. After 10-time MI-2P-SMA, the range of relative errors is significantly reduced, and more than half data points are kept. Therefore, 10 iteration times are selected for this pressure data case.

Compared with the temperature data, the original experimental pressure data have larger error range than the original experimental temperature data. This is due to the higher relative resolution and accuracy of temperature sensing than pressure by this WP-SAW reflective delay line temperature and pressure sensor. The relative resolution and accuracy are related to the sensor node design and the standard of the fabrication processes.

VI. CONCLUSION

The improved MI-2P-SMA method is presented by mathematic deviation from fundamental SMA and traditional 2P-SMA and diagram analysis. The method of selection of the iterative time n is discussed. The WP-SAW reflective delay line temperature and pressure sensor node is briefly introduced. The experimental framework with instrumentation is introduced. The experimental temperature and pressure data and their post-MI-2P-SMA results are compared and discussed by regression and relative error analysis. The results show: the MI-2P-SMA method does not change the original characteristics of experimental data; the more iterative time of MI-2P-SMA applies, the range of relative errors is more significantly reduced; however, at least half data points should be kept after MI-2P-SMA. Therefore, the iterative time n should be less than the number of half data points. The characteristics of original data should also be kept after MI-2P-SMA.

ACKNOWLEDGMENT

The authors would like to thank Dr. Tianli Li from the Shenzhen Key Laboratory of Electromagnetic Control, College of Mechatronics and Control Engineering, Shenzhen University, China.

REFERENCES

[1] T. Wang, H. Luo, W. Jia, A. Liu, and M. Xie, "MTES: An intelligent trust evaluation scheme in sensor-cloud-enabled industrial Internet of Things," *IEEE Trans. Ind. Informat.*, vol. 16, no. 3, pp. 2054–2062, Mar. 2020.

[2] J. Qi, P. Yang, L. Newcombe, X. Peng, Y. Yang, and Z. Zhao, "An overview of data fusion techniques for Internet of Things enabled physical activity recognition and measure," *Inf. Fusion*, vol. 55, pp. 269–280, Mar. 2020.

[3] J. Qi, P. Yang, M. Hanneghan, S. Tang, and B. Zhou, "A hybrid hierarchical framework for gym physical activity recognition and measurement using wearable sensors," *IEEE Internet Things J.*, vol. 6, no. 2, pp. 1384–1393, Apr. 2019.

[4] J. Astill, R. A. Dara, E. D. G. Fraser, B. Roberts, and S. Sharif, "Smart poultry management: Smart sensors, big data, and the Internet of Things," *Comput. Electron. Agricult.*, vol. 170, Mar. 2020, Art. no. 105291.

[5] A. Kamilaris and A. Pitsillides, "Mobile phone computing and the Internet of Things: A survey," *IEEE Internet Things J.*, vol. 3, no. 6, pp. 885–898, Dec. 2016.

[6] X. Liu, K. H. Lam, K. Zhu, C. Zheng, X. Li, Y. Du, C. Liu, and P. W. T. Pong, "Overview of spintronic sensors with Internet of Things for smart living," *IEEE Trans. Magn.*, vol. 55, no. 11, Nov. 2019, Art. no. 0800222.

[7] W.-E. Bulst, G. Fischerauer, and L. Reindl, "State of the art in wireless sensing with surface acoustic waves," *IEEE Trans. Ind. Electron.*, vol. 48, no. 2, pp. 265–271, Apr. 2001.

[8] B. Drafts, "Acoustic wave technology sensors," *IEEE Trans. Microw. Theory Techn.*, vol. 49, no. 4, pp. 795–802, Apr. 2001.

[9] J. W. Grate, S. J. Martin, and R. M. White, "Acoustic wave microsensors," *Anal. Chem.*, vol. 65, pp. 940A–948A, Nov. 1993.

[10] F. Seifert, W.-E. Bulst, and C. Ruppel, "Mechanical sensors based on surface acoustic waves," *Sens. Actuators A, Phys.*, vol. 44, no. 3, pp. 231–239, Sep. 1994.

[11] D. S. Ballantine, R. M. White, S. J. Martin, A. J. Ricco, E. T. Zellers, G. C. Frye, and H. Wohltjen, *Acoustic Wave Sensor—Theory, Design, and Physico-Chemical Applications*. San Diego, CA, USA: Academic, 1997.

[12] A. Pohl, "A review of wireless SAW sensors," *IEEE Trans. Ultrason., Ferroelectr., Freq. Control*, vol. 47, no. 2, pp. 317–332, Mar. 2000.

[13] K. Durdag, "Wireless surface acoustic wave sensors," *Sensors Transducers*, vol. 106, pp. 1–5, Jul. 2009.

[14] D. Malocha, M. Gallagher, B. Fisher, J. Humphries, D. Gallagher, and N. Kozlovski, "A passive wireless multi-sensor SAW technology device and system perspectives," *Sensors*, vol. 13, no. 5, pp. 5897–5922, May 2013.

[15] C. Fu, Y. Ke, M. Li, J. Luo, H. Li, G. Liang, and P. Fan, "Design and implementation of 2.45 GHz passive SAW temperature sensors with BPSK coded RFID configuration," *Sensors*, vol. 17, no. 8, p. 1849, Aug. 2017.

[16] P. Maurya and N. Mandal, "Design analysis of wireless pressure measurement by integrating surface acoustic wave sensor with bourdon tube," *IEEE Sensors J.*, vol. 18, no. 21, pp. 8996–9004, Nov. 2018.

[17] V. Kalinin, A. Leigh, A. Stopps, and S. B. Hanssen, "SAW torque sensor for marine applications," in *Proc. Joint Conf. Eur. Freq. Time Forum IEEE Int. Freq. Control Symp. (EFTF/IFC)*, Besancon, France, Jul. 2017, pp. 347–352.

[18] R. Stoney, D. Geraghty, and G. E. O'Donnell, "Characterization of differentially measured strain using passive wireless surface acoustic wave (SAW) strain sensors," *IEEE Sensors J.*, vol. 14, no. 3, pp. 722–728, Mar. 2014.

[19] L. Rana, R. Gupta, R. Kshetrimayum, M. Tomar, and V. Gupta, "Fabrication of surface acoustic wave based wireless NO_2 gas sensor," *Surf. Coatings Technol.*, vol. 343, pp. 89–92, Jun. 2018.

[20] Y. Wang, M. K. Chyu, and Q.-M. Wang, "Passive wireless surface acoustic wave CO_2 sensor with carbon nanotube nanocomposite as an interface layer," *Sens. Actuators A, Phys.*, vol. 220, pp. 34–44, Dec. 2014.

[21] M. Park and Y. Gao, "Error and performance analysis of MEMS-based inertial sensors with a low-cost GPS receiver," *Sensors*, vol. 8, no. 4, pp. 2240–2261, Mar. 2008.

[22] D. Gebre-Egziabher, G. H. Elkaim, J. D. Powell, and B. W. Parkinson, "Calibration of strapdown magnetometers in magnetic field domain," *J. Aerosp. Eng.*, vol. 19, no. 2, pp. 87–102, Apr. 2006.
[23] P. Batista, C. Silvestre, P. Oliveira, and B. Cardeira, "Accelerometer calibration and dynamic bias and gravity estimation: Analysis, design, and experimental evaluation," *IEEE Trans. Control Syst. Technol.*, vol. 19, no. 5, pp. 1128–1137, Sep. 2011.
[24] K. Diao, Z. Yao, Z. Wang, X. Liu, C. Wang, and Z. Shang, "Investigation of vibration effect on dynamic calibration of pressure sensors based on shock tube system," *Measurement*, vol. 149, Jan. 2020, Art. no. 107015.
[25] R. Kannan and S. Jain, "Adaptive recalibration algorithm for removing sensor errors and its applications in motion tracking," *IEEE Sensors J.*, vol. 18, no. 7, pp. 2916–2924, Apr. 2018.
[26] R. Wei, K. Ouyang, X. Bao, X. Gao, and C. Chen, "High-precision smart calibration system for temperature sensors," *Sens. Actuators A, Phys.*, vol. 297, Oct. 2019, Art. no. 111561.
[27] S. Becker and R. J. Clancy, "Robust least squares for quantized data matrices," *Signal Process.*, vol. 176, Nov. 2020, Art. no. 107711.
[28] Q. Shu, S. Dai, Y. Chen, W. Tan, A. Hu, and P. He, "Research on the surface temperature compensation model of rotary kiln based on polynomial fitting and piecewise correction function," *Infr. Phys. Technol.*, vol. 93, pp. 271–276, Sep. 2018.
[29] J. Luo, Q. Liu, Z. Zhou, and Q. Wei, "The temperature field modeling for metal plate surface based on PSO-B-spline interpolation and FBG sensors," *Measurement*, vol. 159, Jul. 2020, Art. no. 107618.
[30] F. Xu, F. Yang, X. Fan, Z. Huang, and K. L. Tsui, "Extracting degradation trends for roller bearings by using a moving-average stacked auto-encoder and a novel exponential function," *Measurement*, vol. 152, Feb. 2020, Art. no. 107371.
[31] Z. Tang, W. Wu, and J. Gao, "A wireless passive SAW delay line temperature and pressure sensor for monitoring water distribution system," in *Proc. IEEE SENSORS*, New Delhi, India, Oct. 2018, pp. 28–31.
[32] Z. Tang, W. Wu, J. Gao, and P. Yang, "Feasibility study on wireless passive SAW sensor in IoT enabled water distribution system," in *Proc. IEEE Int. Conf. Internet Things (iThings), IEEE Green Comput. Commun. (GreenCom), IEEE Cyber, Phys. Social Comput. (CPSCom), IEEE Smart Data (SmartData)*, Exeter, U.K., Jun. 2017, pp. 830–834.
[33] Z. Tang, W. Wu, and J. Gao, "Water pressure sensingbased on wireless passive SAW technology," *Procedia Eng.*, vol. 119, pp. 892–900, Sep. 2015.

ZHAOZHAO TANG received the B.Eng. degree in electronic science and technology from Xi'an Jiaotong University, Xi'an, China, in 2011, the M.Sc. degree in microelectronics from Newcastle University, Newcastle upon Tyne, U.K., in 2012, and the Ph.D. degree in electrical and electronic engineering from Staffordshire University, Stoke-on-Trent, U.K., in 2019.

He was an Exchange Research Student with the Harbin Institute of Technology, Harbin, China, the Shenzhen Graduate School of Tsinghua University, Shenzhen, China, and the Dalian University of Technology, Dalian, China, under EU FP7 Marie Curie Actions IRSES. He is currently a Postdoctoral Research Fellow with the College of Physics and Optoelectronic Engineering, Shenzhen University, Shenzhen. His research interests include surface acoustic wave sensors and devices, micro- or nanostructured surfaces for chemical and bio-sensors, signal processing, the Internet of Things (IoT), intelligent monitoring, and water distribution systems.

WENYAN WU received the B.Eng. and M.Eng. degrees in electronic engineering from the Dalian University of Technology, Dalian, China, the Ph.D. degree in water quality modeling and optimization in water distribution system from the Harbin Institute of Technology, Harbin, China, in 1999, and the Ph.D. degree from the University of Derby, Derby, U.K., in 2003.

She was a Professor of Digital design and Technologies with Staffordshire University, Stoke-on-Trent, U.K., a Lecturer of Computing with the Harbin Institute of Technology, and a Research Fellow of Water Software Systems with De Montfort University, Leicester, U.K., and the National Key CAD Laboratory, Institute of Computing Technology, Chinese Academy of Sciences, Beijing, China. She is currently a Professor of Smart Sensor and Advanced System Engineering and the Chair in Research Group of Sensor and Actuator with Birmingham City University, Birmingham, U.K. She has extensive research experiences in smart sensors and sensor networks, the IoT, intelligent monitoring, digital design and processing, data visualization and advanced interface, modeling and optimization, water distribution systems, and water resource management. She was a Principle Investigator (PI) and a Project Coordinator of EU FP7-WatERP and EU FP7-SmartWater, EU Horizon 2020-IoT4Win. She has published over 150 science citation index (SCI) journal articles and conference papers. She organized special issue in IEEE journals and regular journal article reviewers for more than ten journals and has co-organized international conferences.

JINLIANG GAO received the B.Eng., M.Eng., and Ph.D. degrees in municipal engineering from the Harbin Institute of Technology, Harbin, China, in 1993, 1996, and 2002, respectively.

He is currently working as an Associate Professor with the School of Environment, Harbin Institute of Technology. He leads a research group and received a variety of research grants as a PI and a co-PI for a number of projects, including EU FP7 Marie Curie Actions, the Royal Society U.K., the National Natural Science Foundation of China, and industries. He has published over 60 articles and contributed contents to three books. He owns five software copyrights and 19 patents. His research interests include water supply network simulation, hydro-informatics, long distance pipeline transient analysis, water supply system optimal schedule, and pipeline hygienics.

JINGTING LUO received the Ph.D. degree from Tsinghua University, China, in 2012.

From 2012 to 2015, he worked as an Assistant Professor with the College of Physics and Technology, Shenzhen University, China. From 2016 to 2017, he worked as an Academic Visitor with the Faculty of Engineering and Environment, University of Northumbria, Newcastle upon Tyne, U.K. Since 2017, he has been an Associate Professor with the College of Physics and Optoelectronic Engineering, Shenzhen University. He has extensive experience in acoustic wave devices, lab-on-chip, micromechanics, piezoelectric thin films, and nanostructured composite/films for applications in MEMS, sensing, and energy harvesting applications. He has published over 100 science citation index (SCI) journal articles and over 20 conference papers. He is regular journal article reviewers for more than ten journals and has co-organized five international conferences.

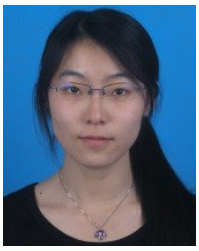

RAN TAO received the B.Eng. degree from Tsinghua University, Beijing, China, in 2011, the dual M.Eng. degree from the École Centrale de Lyon, Université Claude Bernard Lyon 1, and the Institut National des Sciences Appliquées, Lyon, France, in 2013, and the Ph.D. degree from the CNRS, University of Grenoble Alpes, Grenoble INP, Grenoble, France, in 2017.

She worked as a Postdoctoral Researcher with University of Northumbria, Newcastle upon Tyne, U.K., from 2017 to 2020. She is currently working as an Assistant Professor with the College of Physics and Optoelectronic Engineering, Shenzhen University, China. Her research interests include flexible and bendable SAW sensors and acoustofluidics devices.

CHEN FU received the Ph.D. degree from the Chinese Academy of Sciences, China, in 2011.

After his Ph.D., he worked with the MEMS Laboratory, Ajou University, South Korea, and then the Institute of Cellular Medicine, Newcastle University, U.K., respectively. Since 2017, he has been an Assistant Professor with the College of Physics and Optoelectronic Engineering, Shenzhen University, China. His current research interests include theory, design, and fabrication of acoustic MEMS devices.

LUOYUN XU received the B.Eng. degree in electrical and electronic engineering from North China Electric Power University, Beijing, China, in 2015, and the Ph.D. degree in electrical engineering (power system protection and control) from The University of Manchester, U.K., in 2019.

He is currently an Engineer with the Huadian Electric Power Research Institute, China, and a Research Associate with the College of Electrical Engineering, Zhejiang University, China. His research interests include the power system automation and digitalization, energy-storage system management, and optimization for power generation.